Imperfections in Lined Waveguide

By H. L. KREIPE and H. G. UNGER*

(Manuscript received May 11, 1962)

Thickness variations of the lining and deformations of the cross-section couple circular electric waves to unwanted modes and degrade transmission characteristics. Generalized telegraphist's equations for lined waveguide with these imperfections are found. The most critical interaction is caused by lining variations of circular symmetry between TE_{01} and higher circular electric waves. Because of such interaction the average TE_{01} loss is increased and signal transmission is distorted. More serious than signal distortion is the increase in average loss. In 2″ I.D. copper waveguide with a 0.01″ lining, the rms of a typical thickness variation should stay below 0.002″ for the TE_{01} loss at 55.5 kmc not to be raised more than 10 per cent. Cross-sectional deformations in lined waveguide cause nearly the same increase in loss and signal distortion as in plain waveguide. Tolerances for such deformations should therefore be the same as in plain waveguide.

I. INTRODUCTION

Lined waveguide shows promise as a communication medium.[1] Circular electric wave loss in bends is reduced by a low-loss lining. A lossy lining reduces the degrading effects of mode conversion and reconversion.

In straight circular waveguide with a perfectly uniform lining, circular electric waves will only suffer a slight increase in attenuation due to the loss factor of the lining and the slightly increased wall currents. Also, the phase constant will be only slightly shifted. Otherwise the transmission characteristics will remain smooth and undistorted.

A perfect waveguide with a perfectly uniform lining, however, cannot be realized in practice. The waveguide will be slightly deformed, and any lining as it is applied by spraying, dipping, or other methods, will show variations in thickness along the circumference as well as longitudinally. These variations will, in general, be distributed randomly.

* Technische Hochschule Braunschweig; work done under letter contract.

Deformations of the cross section or an imperfect lining couple the circular electric wave to other unwanted modes and by mode conversion and reconversion further increase the loss and otherwise degrade the transmission characteristics. To keep these degrading effects small, the waveguide has to be made sufficiently round and straight and the lining uniform. In order to specify tolerances, a theory is needed of circular electric wave propagation in a deformed waveguide with varying thickness of the lining.

Attempts at such a theory have been made elsewhere, but they were limited to a first-order approximation[2,3,4]. These approximations are by far not adequate to describe the cases of practical interest.

Imperfect lining in a perfect waveguide will be analyzed first. Subsequently, the effects of cross-sectional deformations will be taken into account.

II. GENERALIZED TELEGRAPHIST'S EQUATIONS FOR A WAVEGUIDE WITH IMPERFECT LINING

The lined waveguide, Fig. 1, will be considered in cylindrical coordinates (r, φ, z). The thickness t of the lining will for the moment be assumed a function of φ only. Any such function, being periodic in φ, may be expanded into a Fourier series

$$t = t_1(1 + \sum_q \nu_q \cos q\varphi). \tag{1}$$

The sine terms have been omitted in (1); they would only add terms of orthogonal polarization. t_1 is the nominal thickness of the lining.

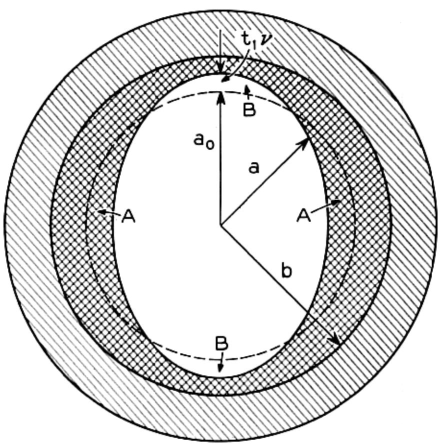

Fig. 1 — Round waveguide with lining of varying thickness.

The relative permittivity will be written

$$\epsilon_1 + \epsilon_2$$

where ϵ_1 is the relative permittivity of the waveguide with a perfectly uniform lining. ϵ_2 takes into account the actual permittivity distribution in a waveguide with varying thickness of the lining.

More specifically:

$$\begin{aligned} \epsilon_1 &= 1 \qquad && 0 < r < a_0 \\ \epsilon_1 &= \epsilon_r \qquad && a_0 < r < b \end{aligned} \tag{2}$$

where ϵ_r is the relative permittivity of the lining. Moreover,

$$\begin{aligned} \epsilon_1 + \epsilon_2 &= \epsilon_r\,; \qquad \epsilon_2 = \epsilon_r - 1 \quad \text{in areas A (Fig. 1)} \\ \epsilon_1 + \epsilon_2 &= 1\,; \qquad \epsilon_2 = 1 - \epsilon_r \quad \text{in areas B.} \end{aligned} \tag{3}$$

In other cross-sectional areas $\epsilon_2 = 0$. Only the thickness of the lining varies; the permittivity is assumed to be constant.

The electromagnetic field in the waveguide is described in terms of normal modes of the round waveguide with a perfectly uniform lining. These modes are derived from two sets of scalar functions T_n and T_n' given by (6.1) and (6.2).*

The transverse field components are written in terms of the following wave functions:

$$\begin{aligned} E_r &= \sum_n V_n \left[\frac{\partial T_n}{\partial r} + d_n \frac{\partial T_n'}{r \partial \varphi} \right] \\ E_\varphi &= \sum_n V_n \left[\frac{\partial T_n}{r \partial \varphi} - d_n \frac{\partial T_n'}{\partial r} \right] \\ H_r &= -\sum_n I_n \left[\frac{\partial T_n}{r \partial \varphi} - d_n \frac{h_n^2}{\epsilon_1 k^2} \frac{\partial T_n'}{\partial r} \right] \epsilon_1 \\ H_\varphi &= \sum_n I_n \left[\frac{\partial T_n}{\partial r} + d_n \frac{h_n^2}{\epsilon_1 k^2} \frac{\partial T_n'}{r \partial \varphi} \right] \epsilon_1 . \end{aligned} \tag{4}$$

The individual terms in (4) represent normal modes of the lined waveguide when d_n is chosen according to (6.26). $k = \omega\sqrt{\mu_0\epsilon_0}$ is the free-space wave number; h_n is the axial propagation constant; and

$$k_n \equiv \chi_n a_0 = a_0(k^2 - h_n^2)^{\frac{1}{2}} \tag{5}$$

is the radial propagation constant of the mode n.

* These equations are listed in Ref. 6; the terminology (6.1) refers to Ref. 6 equation (1), (6.2) to Ref, 6 equation (2), etc.

In Maxwell's equations the distribution of permittivity $(\epsilon_1 + \epsilon_2)$ must be taken into account:

$$\frac{1}{r}\left[\frac{\partial}{\partial\varphi}(E_z) - \frac{\partial}{\partial z}(rE_\varphi)\right] = -j\omega\mu_0 H_r \tag{6}$$

$$\left[\frac{\partial}{\partial z}(E_r) - \frac{\partial}{\partial r}(E_z)\right] = -j\omega\mu_0 H_\varphi \tag{7}$$

$$\frac{1}{r}\left[\frac{\partial}{\partial r}(rE_\varphi) - \frac{\partial}{\partial\varphi}(E_r)\right] = -j\omega\mu_0 H_z \tag{8}$$

$$\frac{1}{r}\left[\frac{\partial}{\partial\varphi}(H_z) - \frac{\partial}{\partial z}(rH_\varphi)\right] = j\omega(\epsilon_1 + \epsilon_2)\epsilon_0 E_r \tag{9}$$

$$\left[\frac{\partial}{\partial z}(H_r) - \frac{\partial}{\partial r}(H_z)\right] = j\omega(\epsilon_1 + \epsilon_2)\epsilon_0 E_\varphi \tag{10}$$

$$\frac{1}{r}\left[\frac{\partial}{\partial r}(rH_\varphi) - \frac{\partial}{\partial\varphi}(H_r)\right] = j\omega(\epsilon_1 + \epsilon_2)\epsilon_0 E_z\,. \tag{11}$$

Substituting for the transverse field components from (4) into (8) and (11) and taking advantage of (6.3), the longitudinal field components are obtained:

$$H_z = j\omega\epsilon_0 \sum_n V_n d_n \frac{\chi_n^2}{k^2} T_n' \tag{12}$$

$$H_z = j\omega\mu_0 \sum_n I_n \frac{\epsilon_1}{\epsilon_1 + \epsilon_2}\frac{\chi_n^2}{k^2} T_n\,. \tag{13}$$

To find relations for the current and voltage coefficients, the series representations (4) and (12) and (13) for the field components are substituted into Maxwell's equations. Then by multiplying with orthogonal field functions, combining some of these equations, and integrating over the cross section, generalized telegraphist's equations are obtained.

For example,

$$-\left(\frac{\partial T_m}{r\partial\varphi} - d_m \frac{h_m^2}{\epsilon_1 k^2}\frac{\partial T_m'}{\partial r}\right)\epsilon_1 \qquad \text{times (6)}$$

is added to

$$\left(\frac{\partial T_m}{\partial r} + d_m \frac{h_m^2}{\epsilon_1 k^2}\frac{\partial T_m'}{r\partial\varphi}\right)\epsilon_1 \qquad \text{times (7)}$$

and the result is integrated over the total cross section. Using the orthonormality condition (6.29)[5] and the wave equation (6.3), one obtains:

$$\frac{dV_m}{dz} + j\,\frac{h_m^{\,2}}{\omega\epsilon_0}\,I_m = -j\omega\mu_0 \sum_n I_n \int_S \frac{\epsilon_1\epsilon_2}{\epsilon_1+\epsilon_2}\,\frac{\chi_n^{\,2}\chi_m^{\,2}}{k^2}\,T_nT_m\,dS. \tag{14}$$

Similarly,

$$-\left(\frac{\partial T_m}{\partial r} + d_m\,\frac{\partial T_m'}{r\partial\varphi}\right) \qquad \text{times (9)}$$

is added to

$$-\left(\frac{\partial T_m}{r\partial\varphi} - d_m\,\frac{\partial T_m'}{\partial r}\right) \qquad \text{times (10)}$$

and the result is integrated over the cross section

$$\begin{aligned}\frac{dI_m}{dz} &+ j\omega\epsilon_0 V_m \\ &= -j\omega\epsilon_0 \sum_n V_n \int_S \epsilon_2\left\{\left[\frac{\partial T_n}{\partial r} + d_n\,\frac{\partial T_n'}{r\partial\varphi}\right]\left[\frac{\partial T_m}{\partial r} + d_m\,\frac{\partial T_m'}{r\partial\varphi}\right]\right. \\ &\qquad \left. + \left[\frac{\partial T_n}{r\partial\varphi} - d_n\,\frac{\partial T_n'}{r\partial r}\right]\left[\frac{\partial T_m}{r\partial\varphi} - d_m\,\frac{\partial T_m'}{\partial r}\right]\right\} dS.\end{aligned} \tag{15}$$

Equations (14) and (15) are generalized telegraphist's equations for round waveguide with imperfect lining.

Introducing traveling waves,

$$\begin{aligned} V_m &= \sqrt{K_m}(a_m + b_m) \\ I_m &= \frac{1}{\sqrt{K_m}}\,(a_m - b_m) \end{aligned} \tag{16}$$

with the characteristic impedance

$$K_m = \frac{h_m}{\omega\epsilon_0}, \tag{17}$$

the more convenient form of generalized telegraphist's equations in terms of amplitudes of forward (a_m) and backward (b_m) traveling waves is obtained:

$$\begin{aligned} \frac{da_m}{dz} + jh_m a_m &= j \sum_n\,[c_{mn}^{\;+}a_n + c_{mn}^{\;-}b_n] \\ \frac{db_m}{dz} - jh_m b_m &= -j \sum_n\,[c_{mn}^{\;+}b_n + c_{mn}^{\;-}a_n]. \end{aligned} \tag{18}$$

The coupling coefficients in (18) are

$$c_{mn}^{\pm} = \mp \frac{k^2}{2\sqrt{h_m h_n}} \int_S \frac{\epsilon_1 \epsilon_2}{\epsilon_1 + \epsilon_2} \frac{\chi_n^2 \chi_m^2}{k^2} T_n T_m \, dS$$
$$- \frac{\sqrt{h_m h_n}}{2} \int_S \epsilon_2 \left\{ \left[\frac{\partial T_n}{\partial r} + d_n \frac{\partial T_n'}{r\partial\varphi} \right] \left[\frac{\partial T_m}{\partial r} + d_m \frac{\partial T_m'}{r\partial\varphi} \right] \right. \tag{19}$$
$$\left. + \left[\frac{\partial T_n}{r\partial\varphi} - d_n \frac{\partial T_n'}{\partial r} \right] \left[\frac{\partial T_m}{r\partial\varphi} - d_m \frac{\partial T_m'}{\partial r} \right] \right\} dS.$$

To analyze circular electric wave propagation, it is sufficient to consider only coupling between circular electric and other waves. Let m denote the TE_{0m} wave, then

$$T_m = 0$$

and

$$E_{z_m} = E_{r_m} = H_{\varphi_m} = 0.$$

In this case the coupling coefficients reduce to

$$c_{mn}^{\pm} = \frac{d_m \sqrt{h_m h_n}}{2} \int_S \epsilon_2 \left[\frac{\partial T_n}{r\partial\varphi} - d_n \frac{\partial T_n'}{\partial r} \right] \frac{\partial T_m'}{\partial r} \, dS. \tag{20}$$

Also the generalized telegraphist's equations may now be written shorter:

$$\begin{aligned} \frac{da_m}{dz} + jh_m a_m &= j \sum_n c_{mn}(a_n + b_n) \\ \frac{db_m}{dz} - jh_m b_m &= j \sum_n c_{mn}(a_n + b_n). \end{aligned} \tag{21}$$

To find the z-dependence of the wave amplitudes a_m and b_m for certain initial conditions requires the solution of the generalized telegraphist's equations (18) or (21). They are a system of simultaneous first-order and linear differential equations and can be solved by standard methods.

III. COUPLING COEFFICIENTS FOR LINING IMPERFECTIONS

First of all, the coupling coefficients have to be evaluated. Under practical conditions certain approximations may be made. The maximum deviation of the lining from its nominal thickness or also any of its Fourier components are assumed to be small compared to the nominal thickness:

$$\nu_p \ll 1. \tag{22}$$

A first approximation is obtained by substituting for the wave functions T_n and T_n' in the range of thickness deviations their values at the nominal boundary $r = a_0$. Thus the integration in (20) is facilitated. ϵ_2 is different from zero only in regions A and B of Fig. 1, and in these regions the integrand is assumed independent of r.

According to the boundary condition at $r = a_0$ for the internal and external field components

$$E_{\varphi_n}{}^i E_{\varphi_m}{}^i = E_{\varphi_n}{}^e E_{\varphi_m}{}^e$$

and consequently, because of (4):

$$\left[\frac{\partial T_n{}^i}{r\partial\varphi} - d_n \frac{\partial T_n{}^{i\prime}}{\partial r}\right]\frac{\partial T_m{}^{i\prime}}{\partial r} = \left[\frac{\partial T_m{}^e}{r\partial\varphi} - d_n \frac{\partial T_n{}^{e\prime}}{\partial r}\right]\frac{\partial T_m{}^{e\prime}}{\partial r}. \tag{23}$$

The various terms of the integrand in (20) are:

$$\begin{aligned} \frac{\partial T_n{}^i}{r\partial\varphi} &= N_n J_p(k_n)\,\frac{p}{a_0}\cos p\varphi \\ \frac{\partial T_n{}^{i\prime}}{\partial r} &= N_n \chi_n J_p'(k_n)\,\cos\,p\varphi \\ \frac{\partial T_m{}^{i\prime}}{\partial r} &= N_m \chi_m J_0'(k_m). \end{aligned} \tag{24}$$

Introducing these terms into (20) and using (23), the coupling coefficients are:

$$c_{mn}{}^{\pm} = \tfrac{1}{2}\sqrt{h_m h_n}\, d_m N_m N_n k_m J_1(k_m) J_p(k_n)(p\text{-}d_n k_n{}^2 y_n) \cdot (\epsilon_r - 1)\,\frac{1}{a_0}\int_0^{2\pi}\int_{a_0}^{b-t}\cos p\varphi\, dr d\varphi \tag{25}$$

$$\text{where } y_n = \frac{J_p'(k_n)}{k_n J_p(k_n)}. \tag{26}$$

Integrating over the radial coordinate r, the upper limit $b - t$ is a function of φ. According to (1)

$$b - t = a_0 - t_1 \sum_q \nu_q \cos q\varphi. \tag{27}$$

Integrating in (25) over r and φ the contributions from all Fourier components of (27) disappear except those with $q = p$. One obtains for the coupling coefficients:

$$c_{mn} = -\tfrac{\pi}{2}\sqrt{h_m h_n}\, d_m N_m N_n k_m J_1(k_m) J_p(k_n)\,(p - d_n k_n{}^2 y_n) \cdot (\epsilon_r - 1)\delta_1 \nu_p \tag{28}$$

where for the nominal thickness the relative measure

$$\delta_1 = \frac{t_1}{a_0} \tag{29}$$

has been introduced.

For a thickness deviation described by a single coefficient ν_p, there is only coupling between circular electric waves and waves of circumferential order $p = q$.

For the term corresponding to $q = 0$ the integration results in

$$c_{mn} = -\pi\sqrt{h_m h_n} d_m N_m d_n N_n k_m k_n J_1(k_m) J_1(k_n)(\epsilon_r - 1)\delta_1 \nu_0. \tag{30}$$

This uniform thickness deviation only causes mutual coupling between circular electric waves.

For a very thin lining, the modes of lined waveguide may be considered perturbed modes of plain waveguide. It has been found elsewhere[6] that a first-order perturbation of this kind is a good approximation only in a very limited range. Nevertheless it will be quite informative to study the approximations for the various expressions when this first-order perturbation is introduced.

The asymmetric modes are either perturbed TE or perturbed TM modes. The coupling coefficient between circular electric and perturbed TE modes reduces to

$$c_{mn} = -\frac{k^2 k_{m0} k_{n0} \left[1 - \dfrac{p^2}{\epsilon_r k_{n0}^2 \dfrac{k^2}{h_{n0}^2}\left(1 + \dfrac{k_{n0}^2}{k^2 b^2(\epsilon_r - 1)}\right)}\right]}{\sqrt{2h_{m0}h_{n0}}\sqrt{1 - \dfrac{p^2}{k_{n0}^2}}} (\epsilon_r - 1)\delta_1^3 \nu_p \tag{31}$$

where the second subscript 0 indicates the value of the corresponding quantity in plain metallic waveguide.

The coupling coefficient between circular electric and perturbed TM modes reduces to

$$c_{mn} = \sqrt{\frac{h_{n0}}{2h_{m0}}}\, k k_{m0} p \frac{\epsilon_r - 1}{\epsilon_r} \delta_1^3 \nu_p . \tag{32}$$

The uniform thickness deviation causes coupling only between circular electric waves. For a very thin lining the corresponding coupling coefficients (30) reduce to

$$c_{mn} = -\frac{k^2 k_{m0} k_{n0}}{\sqrt{h_{m0} h_{n0}}} (\epsilon_r - 1)\delta_1^3 \nu_0 . \tag{33}$$

In all approximate expressions (31) to (33) the coupling coefficients vary with the third power of the relative thickness δ_1 of the lining and are proportional to the relative deviation ν_p of the thickness.

To evaluate the exact expressions (28) and (30) for the coupling coefficients as well as the approximate expressions (31) to (33), the propagation characteristics of the coupled modes must be known first. The characteristic equation for the normal modes in lined waveguide of perfect geometry has been solved numerically by an iterative procedure. The evaluation was programmed for automatic execution on a digital computer.

Also included in this program was an evaluation of the exact formula (28) for coupling between TE_{01} and any asymmetric mode.

For the typical values $b/\lambda = 4.70$ and 7.62 corresponding to 2″ I.D. waveguide at 55.5 kmc and 90 kmc, and for a permittivity $\epsilon_r = 2.5$, the phase constants of a number of modes are plotted versus the relative thickness of the lining in Figs. 2 to 5.

The lining changes phase constants most effectively for TE_{p1} modes and all TM_{pn} modes. All TE_{pn} modes with $n > 1$ show very little change for a thin lining. First-order approximations for the phase constants in case of very thin lining would be represented in these plots by straight lines tangent to the curves at $\delta_1 = 0$. Note that these first-order approximations are gravely in error for most modes and any substantial thickness of the lining.

Some of the coupling coefficients for thickness deviations have been plotted in Figs. 6 to 9 as a function of the thickness of the lining. In the log-log plot of these figures the first-order approximations for thin lining appear as straight lines with slope 3. Note that these straight lines are fairly good approximations for coupling between TE_{01} and TE_{pn} modes with $n > 1$ and a relative thickness of the lining smaller than 1 per cent. For coupling between TE_{01} and all other modes, however, these approximations are again seriously in error.

Note also that coupling between TE_{01} and TE_{pn} modes is always larger than coupling between TE_{01} and TM_{pm} modes. Furthermore, coupling between TE_{01} and TE_{pn} increases with increasing order n of the radial dependence of coupled modes, while it decreases in case of TM_{pn} modes.

In Fig. 10 the coefficients of coupling between TE_{01} and higher circular electric waves for circular symmetric components of lining imperfection corresponding to $p = 0$ have been plotted. First-order approximations for thin linings are shown in this diagram only. They are adequate for the entire thickness range to be considered. As in the general case of

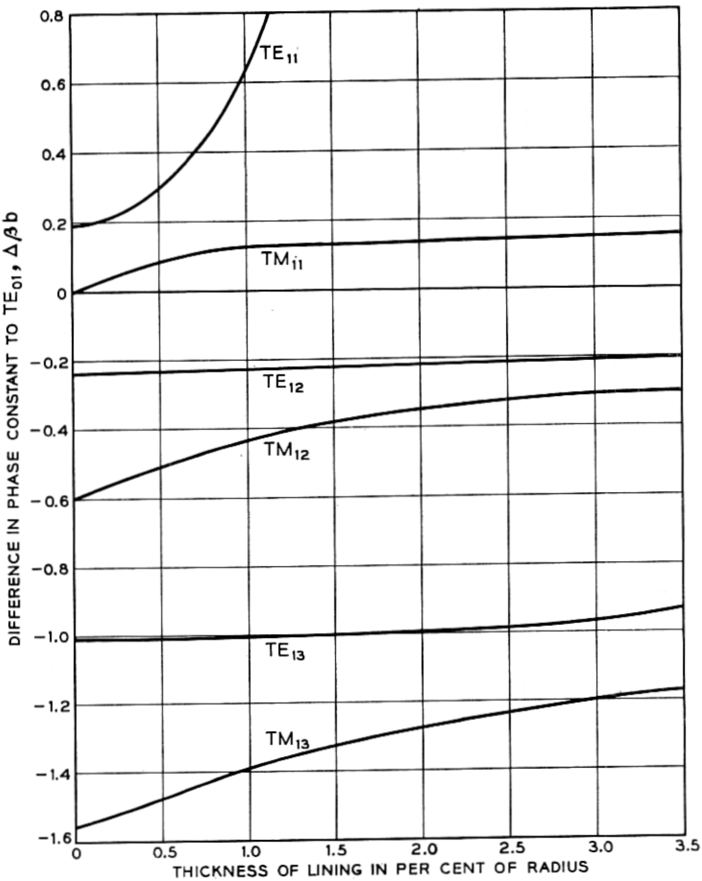

Fig. 2 — Phase constants of TE_{1n} and TM_{1n} modes in lined waveguide. $b/\lambda = 4.70$, $\epsilon_r = 2.5$.

coupling to TE_{pn} the coupling coefficient increases with the radial order n of the higher circular electric modes.

IV. MODE CONVERSION AT IMPERFECT LININGS OF VARIOUS PERMITTIVITIES AND AT VARIOUS FREQUENCIES

Lined waveguide will be used for circular electric wave transmission over wide frequency bands extending up to 100 kmc and more. In addition, for technological reasons the lining might be made of materials of various permittivities.

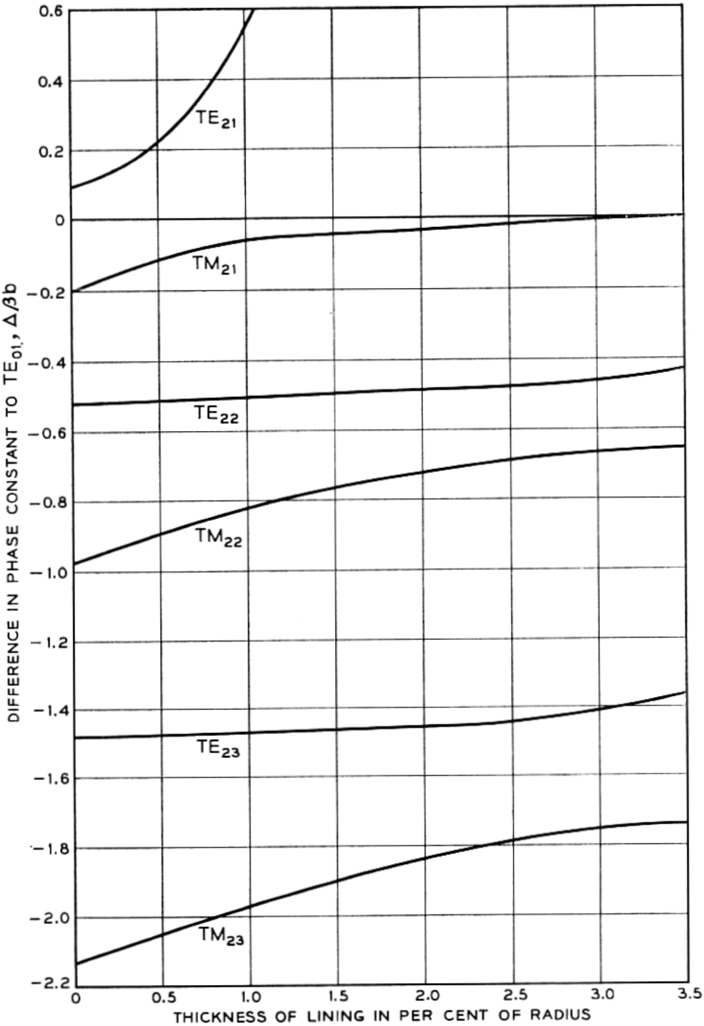

Fig. 3 — Phase constants of TE_{2n} and TM_{2n} modes in lined waveguide. $b/\lambda = 4.70$, $\epsilon_r = 2.5$.

A first indication as to how the coupling coefficients depend on frequency and permittivity of the lining is obtained from the approximate formulae (31), (32) and (33) for coefficients of coupling at lining imperfections.

For interaction between waves which are sufficiently far from cutoff we have

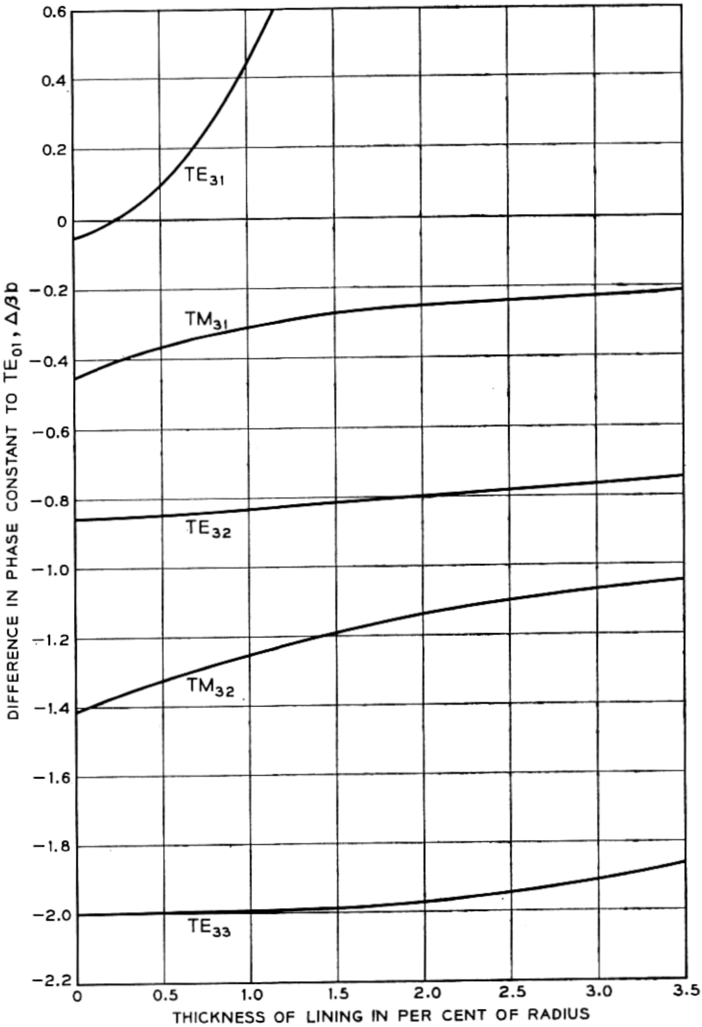

Fig. 4 — Phase constants of TE_{3n} and TM_{3n} modes in lined waveguide. $b/\lambda = 4.70$, $\epsilon_r = 2.5$.

$$h_{m0} \cong h_{n0} \cong k$$

and

$$(\epsilon_r - 1)k^2a^2 \gg k_{n0}^2$$

so that for interaction between TE_{0m} and TE_{pn} (31) may be replaced by

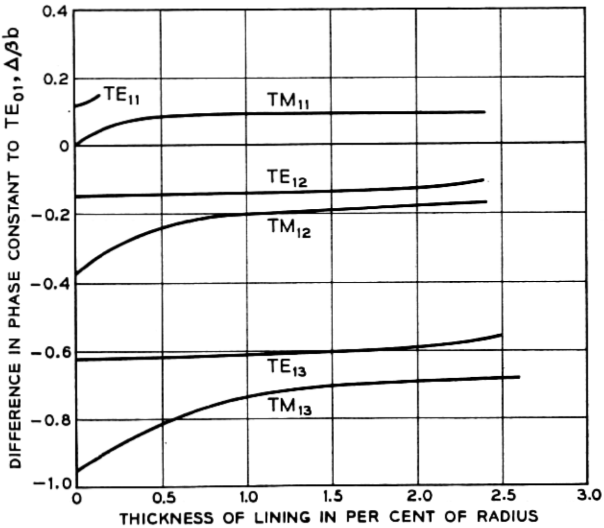

Fig. 5 — Phase constants of TE_{1n} and TM_{1n} modes in lined waveguide. $b/\lambda = 7.62$, $\epsilon_r = 2.5$.

$$c_{mn} = -\frac{k_{n0}k_{m0}}{\sqrt{2}} \frac{1 - \dfrac{p^2}{\epsilon_r k_{n0}^2}}{\left(1 - \dfrac{p^2}{k_{n0}^2}\right)^{\frac{1}{2}}} k(\epsilon_r - 1)\delta_1^{\ 3}\nu_p. \tag{34}$$

Equation (32) for interaction between TE_{0m} and TM_{pn} may be replaced by

$$c_{mn} = \frac{p}{\sqrt{2}} k_{m0} k \frac{\epsilon_r - 1}{\epsilon_r} \delta_1^{\ 3}\nu_p. \tag{35}$$

Equation (33) for interaction between circular electric waves may be replaced by

$$c_{mn} = -k_{m0}k_{n0}k(\epsilon_r - 1)\delta_1^3\nu_0. \tag{36}$$

These approximate expressions indicate a linear dependence on frequency of all coupling coefficients. As functions of the permittivity the coupling coefficients are proportional to $(\epsilon_r - 1)/\epsilon_r$ for interaction between TE_{0m} and TM_{pn} waves, but nearly proportional to $(\epsilon_r - 1)$ for interaction between TE_{0m} and all TE waves. The term $p^2/\epsilon_r k_{n0}^2$ may for most TE modes be neglected with respect to unity.

For substantial linings the normal modes cannot be regarded as per-

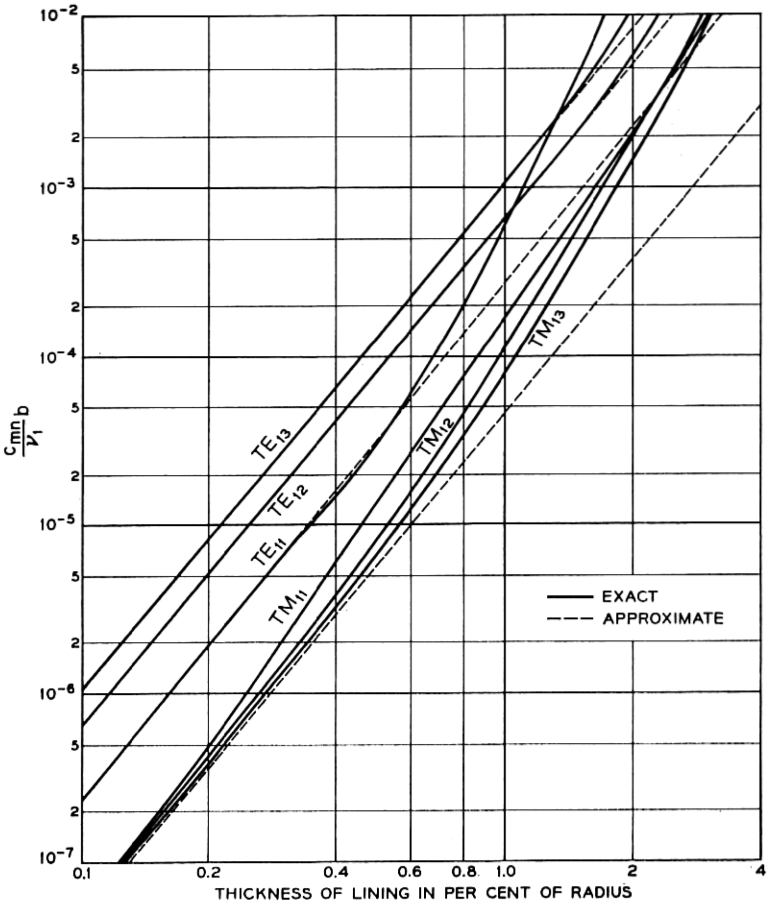

Fig. 6 — Coefficients c_{mn} of coupling between TE_{01} and TE_{1n} and TM_{1n} waves at lining imperfections of order $p = 1$. $b/\lambda = 4.70$, $\epsilon_r = 2.5$.

turbed modes of plain waveguide. In this case an indication of the dependence of mode interaction on permittivity and frequency can be obtained only by evaluating the exact expressions.

Comparing the curves of Figs. 6 and 9, it is found that the exact values for coupling coefficients show nearly the same dependence on frequency and permittivity as indicated by the approximations. Only for interaction between TE_{01} and lower-order TM modes are the coupling coefficients appreciably larger at higher frequencies even for thin linings.

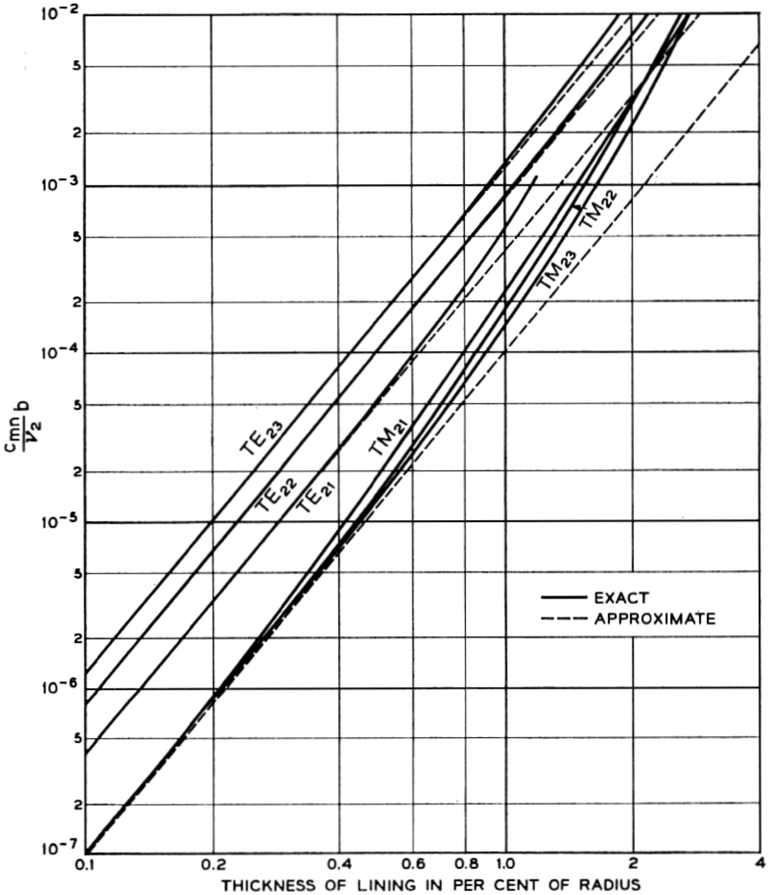

Fig. 7 — Coefficients c_{mn} of coupling between TE_{01} and TE_{2n} and TM_{2n} waves at lining imperfections of order $p = 2$. $b/\lambda = 4.70$, $\epsilon_r = 2.5$.

All these characteristics of coupling due to imperfect linings will have to be considered when the coupled line equations are solved for TE_{01} propagation.

V. LINING TOLERANCES

In manufacturing lined waveguide, tolerances for irregularities must be specified. These irregularities are randomly distributed, and at best some of their statistical properties are known. By solving the generalized

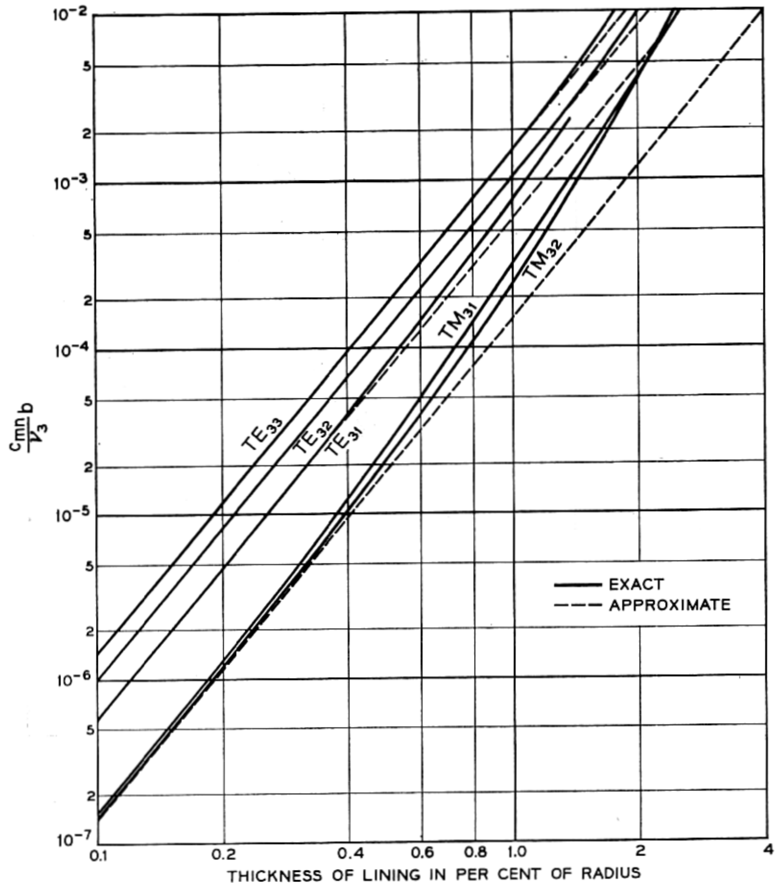

Fig. 8 — Coefficients c_{mn} of coupling between TE_{01} and TE_{3n} and TM_{3n} waves at lining imperfections of order $p = 3$. $b/\lambda = 4.70$, $\epsilon_r = 2.5$.

telegraphist's equations, statistics of the transmission characteristics may be expressed in terms of the statistics of lining imperfections.

In particular, the average added loss for circular electric waves due to mode conversion at lining imperfections is[7]

$$\langle \Delta\alpha_m \rangle = \frac{1}{L} \sum_n \int_0^L R(z)(L - z)\ C_{nm}{}^2 \cos \Delta\beta_{nm} z\, dz \qquad (37)$$

where

$$R(z) = \langle \nu_p(z_1) \cdot \nu_p(z_1 + z) \rangle$$

is the covariance of a component $\nu_p(z)$ of thickness deviation. $\nu_p(z)$ is

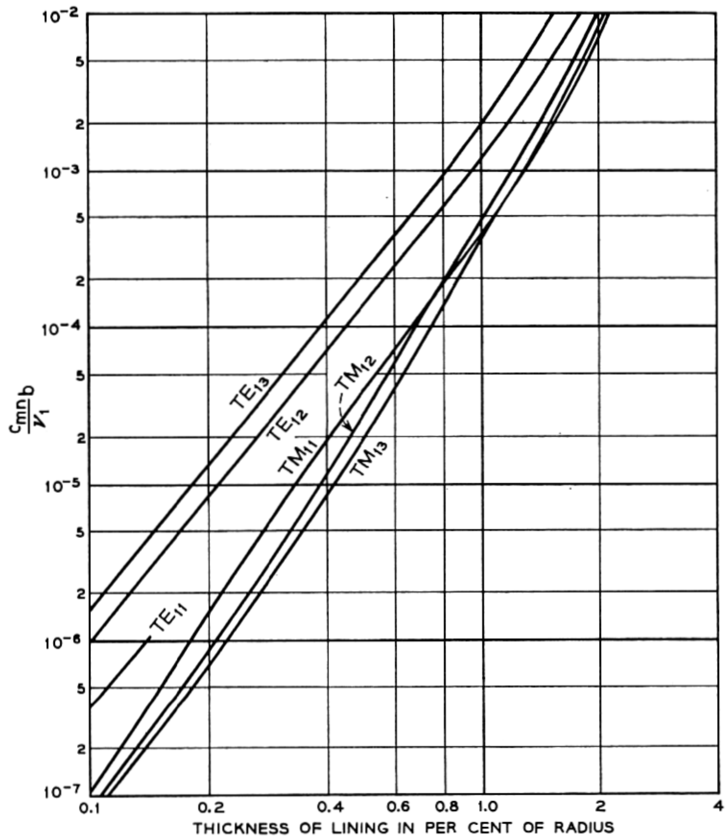

Fig. 9 — Coefficients c_{mn} of coupling between TE_{01} and TE_{1n} and TM_{1n} waves at lining imperfections ($p = 1$). $b/\lambda = 7.62$, $\epsilon_r = 2.5$.

assumed to be a stationary random process in z. C_{nm} is a coupling factor defined according to

$$c_{nm} = C_{nm}\nu_p(z).$$

L is the total length of the waveguide. $\Delta\beta_{nm}$ is the difference in phase constant between the circular electric wave m and the mode n coupled by c_{nm} to m. The difference in attenuation $\Delta\alpha_{nm}$ between mode m and n is assumed small enough so that

$$e^{-\Delta\alpha_{nm}z} \cong 1$$

for all z for which $R(z)$ has any substantial values.

The covariance will be assumed to drop off exponentially

$$R(z) = \langle \nu_p{}^2 \rangle \, e^{-2\pi \frac{|z|}{L_0}} \tag{38}$$

where L_0 is a correlation distance. Substituting (38) for $R(z)$ into (37) and performing the integration for $L_0 \ll L$ the average added loss is:

$$\langle \Delta\alpha_m \rangle = \langle \nu_p{}^2 \rangle \sum_n \frac{2\pi C_{nm}{}^2 L_0}{4\pi^2 + \Delta\beta_{nm}{}^2 L_0{}^2}. \tag{39}$$

To evaluate (39) for the average added loss in the range of relative thickness δ to be considered here, coupling to all TE_{pn} which are propa-

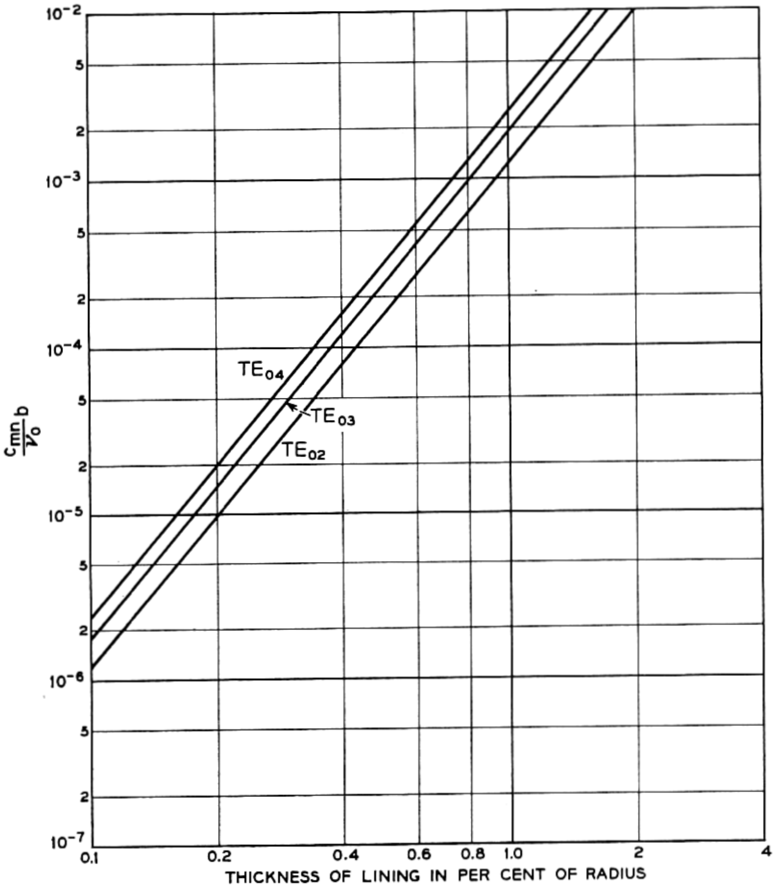

Fig. 10 — Coefficients c_{mn} of coupling between TE_{01} and TE_{0n} waves at lining imperfections of circular symmetry. $b/\lambda = 4.70$, $\epsilon_r = 2.5$.

gating must be taken into account. Of the coupling to TM_{pn} modes only lower-order modes with $n < 4$ need be taken into account. The contribution of coupling to TM_{pn} modes with $n \geqq 4$ to the average added TE_{01} loss is small enough to be neglected.

For the coupling to TE_{pn} modes, first-order approximations for phase constants and coupling coefficients may be used in case of higher-order modes with $n \geqq 4$. The contributions from coupling to these higher-order TE_{pn} modes to the average TE_{01} loss is small enough so that small errors in these approximations will cause no appreciable error in the final result.

For a numerical evaluation of (39) the phase constants of Figs. 2, 3 and 4 and coupling coefficients of Figs. 6, 7, 8 and 10 have been used. For higher-order TE_{pn} modes the approximate expression (31) is adequate. Interaction between circular electric waves at lining imperfections with no circumferential dependence may be described for all modes by approximation (33).

As a result of numerical evaluations, the diagrams in Figs. 11 and 12 have been drawn. They show as a function of the correlation distance L_0 the rms value of ν_p, the particular component of the thickness deviation, which by itself would increase the average TE_{01} loss by 1 per cent

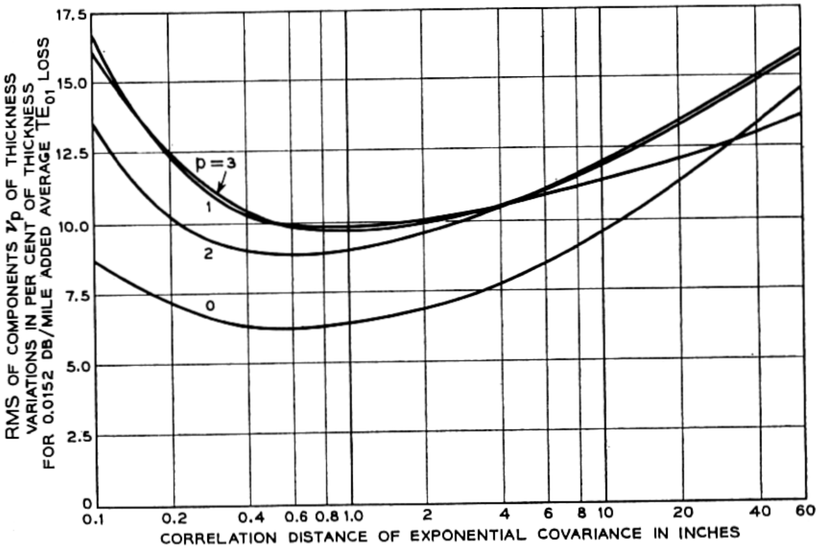

Fig. 11 — TE_{01} loss in lined waveguide with random lining imperfections of exponential covariance: 2-inch inside diameter, at 55.5 kmc, lining $\epsilon_r = 2.5$, $\delta =$ 1 per cent.

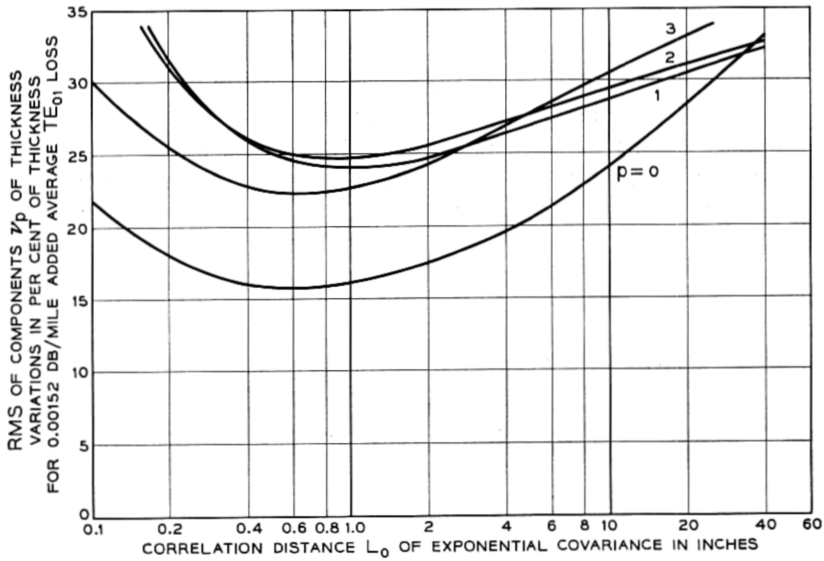

Fig. 12 — TE_{01} loss in lined waveguide with random lining imperfections of exponential covariance: 2-inch inside diameter at 55.5 kmc, lining $\epsilon_r = 2.5$, $\delta = 0.5$ per cent.

in Fig. 11 and 0.1 per cent in Fig. 12 of its value in perfect copper waveguide.

All curves show a minimum. Among all the ν_p the strictest tolerance is imposed on ν_0 by the interaction between circular electric waves. In this case for the critical correlation distance $L_0 = 0.6''$ the rms of thickness deviations of a lining of $\delta = 1$ per cent should, according to Fig. 11, be less than 6 per cent. In absolute values the 0.01″ thick lining should be made uniform to ±0.0006″.

When the lining is thinner, the tolerances are considerably eased. According to Fig. 12 and noting that the extra loss varies as the square of the thickness deviations, a 0.005″ thick lining needs only to be made uniform to ±0.0025″ for the circular electric wave interaction to increase the average TE_{01} loss not more than by 1 per cent.

Mode interaction at lining imperfections not only increases the average TE_{01} loss, but also degrades the transmission characteristics which in perfect waveguide would be smooth functions of frequency. Signals transmitted through imperfect waveguide will suffer amplitude and phase distortion.

A radio-frequency pulse of rectangular shape might be considered a standard signal. Mode conversion-reconversion effects will cause reconversion forerunners to precede the output pulse and tails to follow it.[8] If too large in amplitude, these forerunners and tails will in a *PCM* system produce errors in regeneration.

The *rms* amplitude of the reconversion tail is largest after a long signal pulse. Immediately after this pulse, the contribution to the rms value by reconversion from one coupled mode is given by[9]

$$\sqrt{\overline{|q|^2}} = C_{mn}^{\ 2}\,\varphi(\Delta\beta_{mn})\sqrt{\frac{L}{2\Delta\alpha_{mn}}}\,. \tag{40}$$

In (40) $\Delta\alpha_{mn}$ is the difference in attenuation constant between TE_{0m} and the coupled mode n. φ is the spectral distribution of ν_p given in terms of the covariance by

$$\varphi(\xi) = \int_{-\infty}^{+\infty} R(z)e^{-j\xi z}\,dz. \tag{41}$$

For the exponential covariance of (38) the spectral distribution is

$$\varphi(\xi) = \langle\nu_p^{\ 2}\rangle\,\frac{4\pi L_0}{4\pi^2 + \xi^2 L_0^{\ 2}}\,. \tag{42}$$

The contributions to the reconversion tail from different modes are caused by components of the spectral distribution $\varphi(\xi)$ at the corresponding $\xi = \Delta\beta_{mn}$. From one coupled mode to the next these are quite different spectral components. Their contributions might therefore be assumed to be uncorrelated. Then the total contribution to the rms value is obtained from the sum of the squares of each single contribution:

$$\overline{|q_t|^2} = \sum_n C_{mn}^{\ 4}\,\varphi^2(\Delta\beta_{mn})\,\frac{L}{2\Delta\alpha_{mn}}\,. \tag{43}$$

The most critical signal distortion will undoubtedly be caused by circular electric wave interaction at lining imperfections of order $p = 0$. Not only does this interaction increase the average TE_{01} loss most strongly, but higher circular electric waves are also propagating with extremely low loss. They will, therefore, contribute terms to the sum of (43) which are large because the denominator $\Delta\alpha_{mn}$ is small. Signal distortion due to circular electric wave interaction should therefore be considered first.

In Fig. 13 the quantity $\dfrac{|\overline{q_t^2}|}{L\,\overline{\nu_0^{\ 2}}}$ has been plotted as a function of the correlation distance L_0. Mode interaction between TE_{01} and TE_{02} contributes most strongly to the reconversion tail. Therefore the curve has a maximum where the $TE_{01} - TE_{02}$ term in (43) has its maximum value. Since in (42) the spectral distribution assumes its largest value when $L_0 = \frac{2\pi}{\xi}$, the terms in (43) will show their largest value when

$$L_0 = \frac{2\pi}{\Delta\beta_{mn}}$$

that is, when the correlation distance is equal to the beat wavelength between the two coupled modes. In Fig. 13 the maximum occurs at the beat wavelength between TE_{01} and TE_{02}.

For this most critical spectral distribution of random imperfections the total reconversion tail is still quite small. For example, let $\sqrt{\overline{\nu_0^2}} = 0.2$ be the rms of thickness deviations; then for a waveguide length of $L = 20$ miles the rms of the reconversion tail amplitude is still more than 30 db down compared to the signal pulse. Tolerances on lining imperfections, therefore, need not be as strict for signal distortion as they must be for the increase in average TE_{01} loss. In the present example the increase in average TE_{01} loss would be nearly 4 per cent.

At higher frequencies an increase of mode conversion is indicated by the linear frequency dependence of coupling coefficients according to

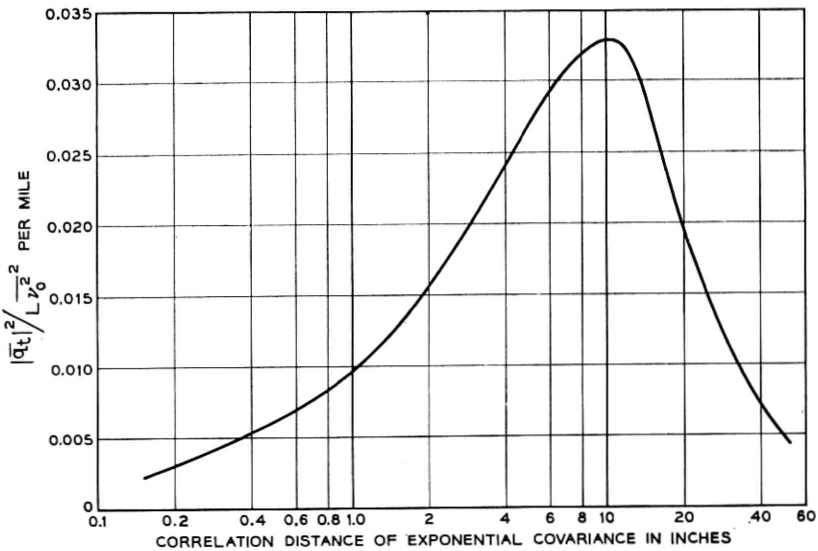

Fig. 13 — TE_{01} — pulse distortion in lined waveguide with random imperfections of the lining. Mode conversion causes a reconversion tail of rms amplitude $\sqrt{\overline{|q_t|^2}}$ to follow the pulse. $b/\lambda = 4.70$, $\epsilon_r = 2.5$, $\delta = 1$ per cent.

(34), (35) and (36). In addition the beat wavelength between coupled modes increases linearly with frequency. The coupling coefficients will also be larger for higher permittivities of the lining.

For operation at higher frequencies or with linings of larger permittivities, tolerances will have to be chosen correspondingly tighter.

VI. GENERALIZED TELEGRAPHIST'S EQUATIONS FOR DEFORMED WAVEGUIDE

Cross-sectional deformations of the lined waveguide will couple circular electric waves to unwanted modes and like imperfections of the lining degrade the transmission by mode conversion and reconversion.

To analyze wave propagation in deformed waveguide, a wall impedance representation will be used to formulate the boundary conditions at the surface of the lining.[6] In perfectly normal waveguide the boundary conditions of a perfectly uniform lining are

$$E_z = -Z_z H_\varphi \tag{44}$$

$$E_\varphi = Z_\varphi H_z . \tag{45}$$

Small deformations cause the radius a of Fig. 14 to be a function of φ,

$$a = a_0[1 + \sigma(\varphi)]. \tag{46}$$

Any function σ, being periodic in φ, may be expanded into a Fourier series:

$$a = a_0[1 + \Sigma_q \sigma_q \cos q\varphi]. \tag{47}$$

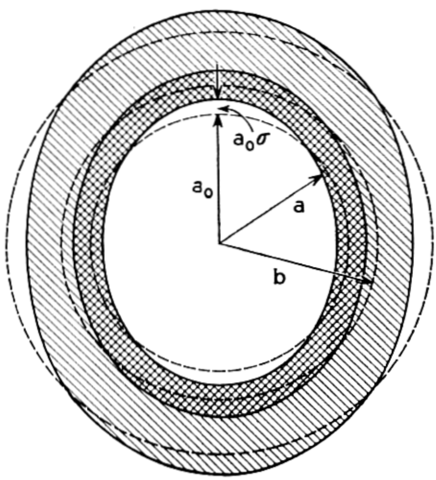

Fig. 14 — Lined waveguide with cross-sectional deformation.

Sine terms have been omitted; they would only add terms of orthogonal polarization. The deformation is assumed to be small and smooth:

$$\sigma \ll 1, \qquad \frac{d\sigma}{d\varphi} \ll 1. \tag{48}$$

For the deformed waveguide the boundary conditions will now have to be satisfied at $r = a$ and not at the nominal radius a_0. In (44) and (45) the tangential components of the magnetic field require the tangential electric field to have a certain value. The magnetic field may be considered to excite the electric field. In the deformed waveguide this excitation stays nearly the same, but due to the slight displacement of the wall it now occurs at $r = a$.

The electric field at $r = a$ can by Taylor series expansion be written in terms of the field at $r = a_0$. Neglecting higher-order terms

$$E(a) = E(a_0) + \frac{\partial E(a_0)}{\partial r} a_0\sigma \tag{49}$$

and the boundary conditions are:

$$E_z(a_0) + \frac{\partial E_z(a_0)}{\partial r} a_0\sigma = -Z_z H_\varphi(a_0) \tag{50}$$

$$E_\varphi(a_0) + \frac{\partial E_\varphi(a_0)}{\partial r} a_0\sigma + E_r(a_0)\frac{d\sigma}{d\varphi} = Z_\varphi H_z(a_0). \tag{51}$$

Maxwell's equations for $r < a$ are given by (6) to (11) with $\epsilon_1 + \epsilon_2 = 1$. Also, the representation of the transverse field components for $r < a$ in terms of normal modes of the perfect lined waveguide is as in (4). Substituting for the transverse field components from (4) into (11), the longitudinal electric field is obtained:

$$E_z = j\omega\mu_0 \sum_n I_n \frac{\chi_n^2}{k^2} T_n . \tag{52}$$

The longitudinal magnetic field, however, cannot be obtained from (8) since the series expression for E_φ in (4) is nonuniformly convergent and must not be substituted for differentiation into (8). We only substitute for E_r from (4), multiply (8) by T_m', and integrate over the cross section. After partial integration:

$$-j\omega\mu_0 \int_s H_z T_m' \, dS = \int_0^{2\pi} E_\varphi T_m' a_0 d\varphi \tag{53}$$
$$- \sum_n V_n \int_0^{2\pi} T_m' \left[\frac{\partial T_n'}{r\partial\varphi} - d_n \frac{\partial T_n'}{\partial r}\right] a_0 \, d\varphi + \sum_n V_n d_n x_n^2 \int_S T_n' T_m' \, dS.$$

To find relations for the current and voltage coefficients, substitute (4) for the field components into Maxwell's equations. Then add

$$-\frac{\partial T_m}{r\partial\varphi} + d_m \frac{h_m^2}{k^2} \frac{\partial T_m'}{\partial r} \quad \text{times (6)}$$

and

$$\frac{\partial T_m}{\partial r} + d_m \frac{h_m^2}{k^2} \frac{\partial T_m'}{r\partial\varphi} \quad \text{times (7)}$$

and integrate over the nominal cross section. The result is

$$\begin{aligned}\frac{dV_m}{dz} + j\frac{h_n^2}{\omega\epsilon_0} I_m = \int_S (\text{grad } E_z)(\text{grad } T_m)\, dS \\ + d_m \frac{h_m^2}{k^2} \int_S (\text{grad } E_z)(\text{flux } T_m')\, dS \\ - j\omega\mu_0 \sum_n I_n \frac{\chi_n^2}{k^2} \Big[\int_S (\text{grad } T_n)(\text{grad } T_m)\, dS \\ + d_m \frac{h_m^2}{k^2} \int_S (\text{grad } T_n)(\text{flux } T_m')\, dS. \end{aligned} \tag{54}$$

After partial integration on the right-hand side of (54),

$$\begin{aligned}\frac{dV_m}{dz} + j\frac{h_m^2}{\omega\epsilon_0} I_m = \int_0^{2\pi} E_z \left(\frac{\partial T_m'}{\partial r} + \frac{d_m}{a_0} \frac{h_m^2}{k^2} \frac{\partial T_m'}{\partial\varphi} \right) a_0 d\varphi \\ + \chi_m^2 \int_S E_z T_m\, dS - j\omega\mu_0 \sum_n I_n \frac{\chi_n^2}{k^2} \left[\int_0^{2\pi} T_n \left(\frac{\partial T_m}{\partial r} + \frac{d_m}{a_0} \frac{h_m^2}{k^2} \frac{\partial T_m'}{\partial\varphi} \right) a_0\, d\varphi \right. \\ \left. + \chi_m^2 \int_S T_n T_m'\, dS \right]. \end{aligned} \tag{55}$$

In special cases when the lining is very thin or when there is no lining, the individual terms for E_z in (52) are zero for $r = a_0$, while E_z itself, because of the boundary condition (50), is different from zero. Then (50) is a nonuniformly convergent series, which describes E_z only in the open interval $0 < r < a_0$. Term-by-term differentiation will make the series diverge. Therefore the series had not been substituted for E_z in (54). In (55) it may now be substituted in the integral over the cross section. In the line integral, E_z from the boundary condition (50) may be substituted. Thus, instead of (55),

$$\frac{dV_m}{dz} + j\frac{h_m^2}{\omega\epsilon_0} I_m = -a_0 \int_0^{2\pi} a_0\sigma \frac{\partial E_z}{\partial r} \left[\frac{\partial T_m}{\partial r} + \frac{d_m}{a_0} \frac{h_m^2}{k^2} \frac{\partial T_m'}{\partial\varphi} \right] d\varphi. \tag{56}$$

Similarly, add

$$-\left(\frac{\partial T_m}{\partial r} + \frac{d_m}{r}\frac{\partial T_m'}{\partial \varphi}\right) \quad \text{times (9)}$$

$$-\left(\frac{1}{r}\frac{\partial T_m}{\partial \varphi} - d_m \frac{\partial T_m'}{\partial r}\right) \quad \text{times (10)}$$

and integrate over the cross section. The result is

$$\begin{aligned}\frac{dI_m}{dz} + j\omega\epsilon_0 V_m = {} & -a_0 \int_0^{2\pi} H_z \left(\frac{\partial T_m}{r\partial\varphi} - d_m \frac{\partial T_m'}{\partial r}\right) d\varphi \\ & + d_m \int_S \chi_m^2 H_z T_m' dS + j\omega\epsilon_0 \sum_n V_n d_n \frac{\chi_n^2}{k^2} \qquad (57) \\ & \cdot\left[a_0 \int_0^{2\pi} T_n' \left(\frac{\partial T_m}{r\partial\varphi} - d_m \frac{\partial T_m'}{\partial r}\right) d\varphi - d_m \int_S \chi_m^2 T_n' T_m' dS\right].\end{aligned}$$

The boundary condition $E_{\varphi n} = Z_\varphi H_{zn}$ of the perfect waveguide may be used for the normal mode term $\left(\frac{\partial T_n}{r\partial\varphi} - d_n \frac{\partial T_n'}{\partial r}\right)$ in (53) and (57), and (53) may be substituted into (57). The result is

$$\frac{dI_m}{dz} + j\omega\epsilon_0 V_m = -j\omega\epsilon_0 a_0 d_m \frac{\chi_m^2}{k^2} \int_0^{2\pi} T_m' [E_\varphi - Z_\varphi H_z] \, d\varphi. \quad (58)$$

Introducing the boundary condition (51) for E_φ we get instead of (58)

$$\frac{dI_m}{dz} + j\omega\epsilon_0 V_m = -j\omega\epsilon_0 a_0 d_m \frac{\chi_m^2}{k^2} \int_0^{2\pi} T_m' \left[a_0 \sigma \frac{\partial E_\varphi}{\partial r} + \frac{d\sigma}{d\varphi} E_r\right] d\varphi. \quad (59)$$

Partially integrating the last term under the integral

$$\int_0^{2\pi} T_m' \frac{d\sigma}{d\varphi} E_r d\varphi = -\int_0^{2\pi} \sigma \left[\frac{\partial E_r}{\partial\varphi} T_m' + E_r \frac{\partial T_m'}{\partial\varphi}\right] d\varphi$$

and substituting for E_r and E_φ from (4) and for $\left[\frac{1}{a_0}\frac{\partial T_n}{\partial\varphi} - d_n \frac{\partial T_n'}{\partial\varphi}\right]$ from the boundary condition in perfect waveguide, the other set of generalized telegraphist's equations is obtained:

$$\begin{aligned}\frac{dI_m}{dz} + j\omega\epsilon_0 V_m = {} & j\frac{a_0}{\omega\mu_0} d_m \chi_m^2 \int_0^{2\pi} E_r \frac{\partial T_m'}{\partial\varphi} \sigma d\varphi - j \sum_n V_n d_n d_m \frac{k_n^2 k_m^2}{\omega\mu_0 a_0^2} \qquad (60) \\ & \cdot \int_0^{2\pi} \left[1 - j\frac{Z\varphi}{\omega\mu_0 a_0}\right] T_n' T_m' \sigma d\varphi.\end{aligned}$$

The interest is limited here to propagation characteristics of circular electric waves. Therefore, only terms that describe direct interaction between circular electric and other waves need to be retained in (56) and (60). When V_m and I_m are amplitudes of other modes, then E_z, H_φ and E_r of circular electric waves are zero. Thus (56) and (60) reduce to

$$\frac{dV_m}{dz} + j\frac{h_m^2}{\omega\epsilon_0} I_m = 0$$

$$\frac{dI_m}{dz} + j\omega\epsilon_0 V_m = -j \sum_n V_n d_n d_m \frac{k_n^2 k_m^2}{\omega\mu_0 a_0^2}\left(1 - j\frac{Z\varphi}{a_0\omega\mu_0}\right)\int_0^{2\pi} \sigma T_n' T_m' d\varphi. \tag{61}$$

Introducing traveling waves as in (16) and (17), the more convenient form (18) of generalized telegraphist's equations is obtained.

The coupling coefficients are

$$c_{nm}^{\pm} = \frac{1}{2}\sqrt{h_n h_m}\, d_n d_m \frac{k_n^2 k_m^2}{k^2 a_0^2}\left(1 - j\frac{z_\varphi}{k a_0}\right)\int_0^{2\pi} \sigma T_n' T_m'\, d\varphi \tag{62}$$

where $z_\varphi = \sqrt{\epsilon_0/\mu_0}\, Z_\varphi$ is the wall impedance with respect to free space.

Substituting from (6.1) for T_n and T_n' and from (47) for $\sigma(\varphi)$,

$$c_{nm}^{\pm} = \frac{\pi}{2}\sqrt{h_n h_m}\, d_n d_m \frac{k_n^2 k_m^2}{k^2 a_0^2} N_n N_m J_0(k_n) J_p(k_m)\sigma_p \left(1 - j\frac{z_\varphi}{k a_0}\right). \tag{63}$$

A component σ_p causes coupling only between circular electric waves and waves of circumferential order p.

The wall impedance in (63) may for all cases of present interest be approximated by:

$$z_\varphi = \frac{1}{\sqrt{\epsilon_r - 1}} \tan k a_0 \sqrt{\epsilon_r - 1}\, \delta_1 . \tag{64}$$

For a very thin lining the expression (63) for the coupling coefficients reduces to the coefficient for coupling at the corresponding deformation in plain metallic waveguide. We obtain $c_{nm} = 0$ for interaction between TE_{0m} and TM_{pn}. For interaction between TE_{0m} and TE_{pn} the coupling coefficients are

$$c_{[0m][pn]} = \frac{k_{m0} k_{n0}}{a_0^2\sqrt{2h_{m0}h_{n0}}} \frac{k_{n0}}{\sqrt{k_{n0}^2 - p^2}} \sigma_p . \tag{65}$$

The numerical evaluation of the general expression (63) has been included in the program for automatic execution. Typical results have been plotted in Fig. 15 for a waveguide with a continuous axial offset ($p = 1$),

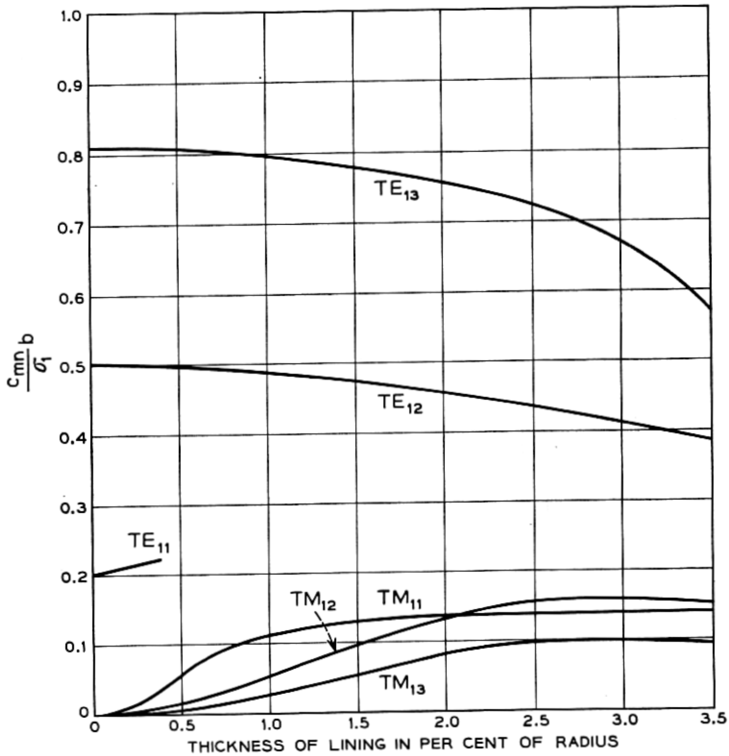

Fig. 15 — Coefficients c_{mn} of coupling between TE_{01} and TE_{1n} and TM_{1n} in axially offset lined waveguide. $b/\lambda = 4.70$, $\epsilon_r = 2.5$.

in Fig. 16 for elliptical deformation, and in Fig. 17 for trifoil deformation.

In all three cases the coupling coefficients have the following characteristics in common: The coupling between TE_{01} and TM waves is much weaker than the coupling between TE_{01} and TE waves even for a substantial thickness of the lining. For a particular deformation the coefficient of coupling between TE_{01} and TE_{pn} waves increases with the index n of the waves. Higher-order waves are coupled more strongly. The relative change of coupling between TE_{01} and TE_{pn} with the thickness of the lining is only slight in particular for coupling to higher-order waves.

The most significant consequence of these general characteristics is that mode conversion effects due to coupling at waveguide deformations will be nearly the same in lined waveguide as they are in plain wave-

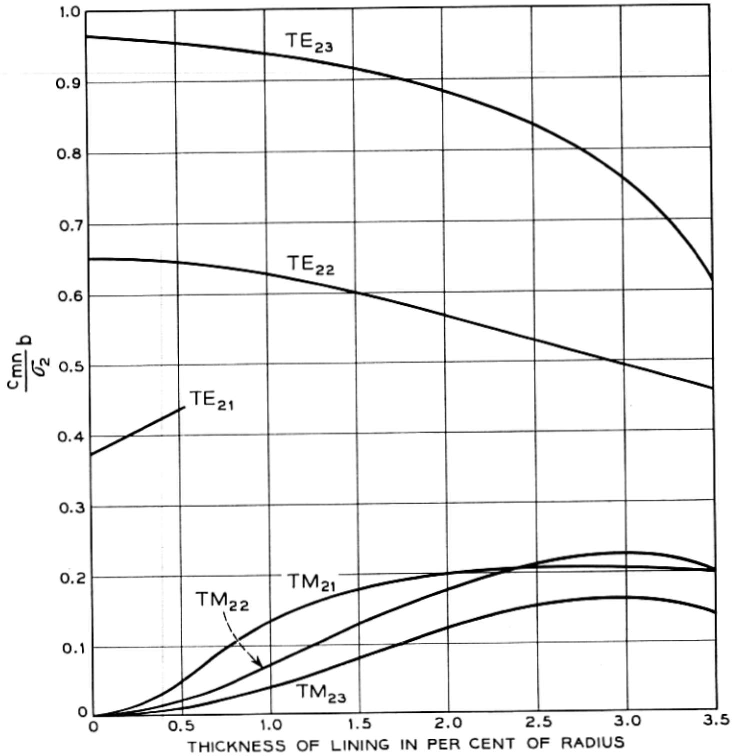

Fig. 16 — Coefficients c_{mn} of coupling between TE_{01} and TE_{2n} and TM_{2n} in lined waveguide with elliptical deformation. $b/\lambda = 4.70$, $\epsilon_r = 2.5$.

guide. Lined waveguide should therefore be manufactured to the same cross-sectional tolerances as is plain waveguide.

VII. CONCLUSIONS

TE_{01} transmission in lined waveguide is degraded by thickness variations of the lining and cross-sectional deformations. These imperfections couple the TE_{01} wave to unwanted modes. The coupling to higher circular electric waves at thickness variations of circular symmetry is strongest. Asymmetric thickness variations couple TE_{01} to the corresponding asymmetric modes.

Random thickness variations increase the average TE_{01} loss and cause signal distortion. The increase in loss is much more pronounced than signal distortion. In a typical example of random thickness variations of

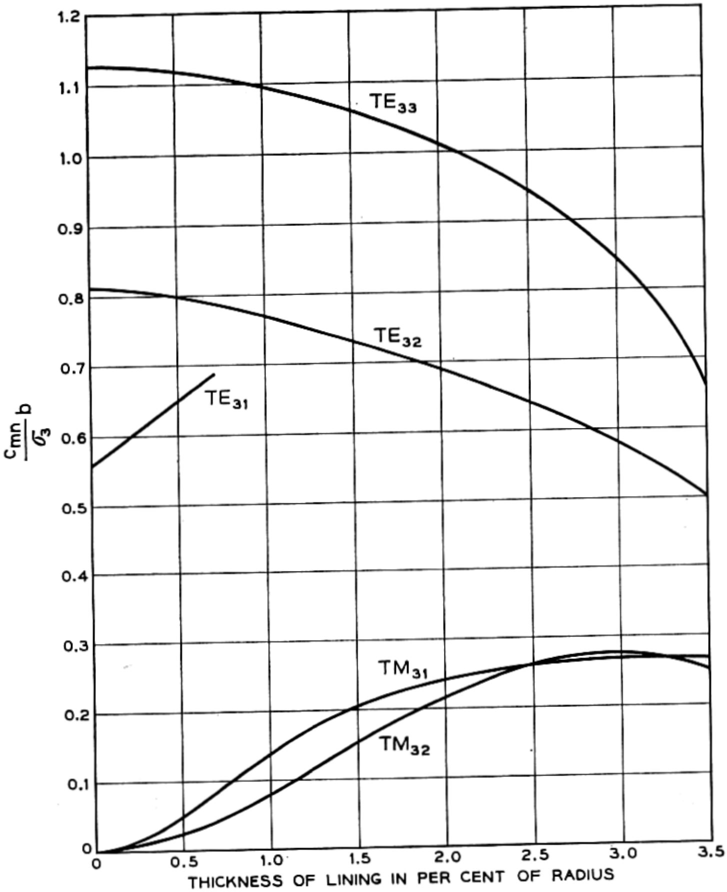

Fig. 17 — Coefficients c_{mn} of coupling between TE_{01} and TE_{3n} and TM_{3n} in lined waveguide with trifoil deformation. $b/\lambda = 4.70$, $\epsilon_r = 2.5$.

a 0.01″ lining of $\epsilon = 2.5$ in a 2″ I.D. waveguide at 55.5 kmc, the rms of the symmetric component of this variation should remain smaller than 0.002″ for the average TE_{01} loss, not to be raised by more than 10 per cent of its value in perfect copper pipe. Under these conditions a pulse signal after traveling through 20 miles of this waveguide is distorted only by a reconversion tail nearly 30 db smaller than the signal. The signal distortion, being caused by circular electric wave interaction, can not, however, be reduced by ordinary mode filters.

Cross-sectional deformations in lined waveguide cause nearly the same interaction of TE_{01} with unwanted modes as corresponding deformations in plain waveguide. Lined waveguide should be manufactured to the same cross-sectional tolerances as plain waveguide.

REFERENCES

1. Unger, H. G., Circular Electric Wave Transmission in a Dielectric Coated Waveguide, B. S. T. J. **36,** September, 1957, pp. 1253–1278.
2. Katsenelenbaum, B. Z., The Effect of a Dielectric Film on the Attenuation of H_{01} Waves in a Straight Nearly Circular Waveguide, Radiotekhnika i Elektronika, 1958, pp. 38–45.
3. Noda, Ken-ichi, Circular Electric Wave Transmission through Hybrid-Mode Waveguide, Review of the Electrical Communications Lab. (Tokyo) **8,** Nos. 9–10, 1960.
4. Janssen, W., Bestimmung der Modenumwandlung im Rundhohlleiter mit unregelmässigem dielektrischen Belag. Archiv Elektr. Übertragung **15,** 1961, pp. 525–536.
5. Bressler, A. D., Joshi, G. H., Marcuvitz, N., Orthogonality Properties for Modes in Passive and Active Uniform Waveguides, J. Appl. Phys. **29,** pp. 794–799.
6. Unger, H. G., Lined Waveguide, B. S. T. J., **41,** March, 1962, pp. 745–768.
7. Rowe, H. E., and Warters, W. D., Transmission in Multimode Waveguide with Random Imperfections, B. S. T. J., **41,** May, 1962, pp. 1031–1170.
8. Miller, S. E., Waveguide as a Communication Medium, B. S. T. J., **33,** November, 1954, pp. 1209–1265.
9. Unger, H. G. Regellose Störungen in Wellenleitern, Archiv Elektr., Übertragung **15,** pp. 393–401 (1961).